

$^{92,94,97,98}\text{Mo}(t,p)$ reactions at $E_t = 17$ MeV

E. R. Flynn, F. Ajzenberg-Selove,* Ronald E. Brown, J. A. Cizewski,[†] and J. W. Sunier
Los Alamos National Laboratory, Los Alamos, New Mexico 87545

(Received 23 July 1981)

A systematic study of the molybdenum isotopes has been carried out by using the (t,p) reaction with a 17-MeV incident triton beam. Energy levels up to excitation energies of 5.1, 4.7, 2.1, and 3.8 MeV in the isotopes $A = 94, 96, 99$, and 100, respectively, were studied, and numerous spin assignments were made. Of particular interest is the trend of ground state and excited 0^+ state transition strengths, which suggest a rapidly changing structure of the molybdenum ground states as a function of neutron number. The interacting boson approximation model is able to reproduce these trends only with the introduction of configuration mixing.

[NUCLEAR REACTIONS $^{92,94,97,98}\text{Mo}(t,p)$ measured $\sigma(\theta)$ DWBA]
 analysis.

I. INTRODUCTION

The molybdenum isotopes represent a system of nuclei which undergoes a significant change in structure as a function of neutron number. The lightest isotopes exhibit a rather simple shell model behavior near the closed neutron shell at $N = 50$ in ^{92}Mo . The heavier nuclei, with $N \gtrsim 60$ appear to be undergoing some type of phase transition, with decay scheme data from fission fragments suggesting the occurrence of a shape deformation. It is possible to investigate these features over a large range of nuclei by using the two nucleon transfer reaction (t,p) to determine the systematic trend and magnitude of the transition away from simple shell model behavior toward a deformed collective structure.

We have combined our present (t,p) reaction studies at 17 MeV on targets of $^{92,94,97,98}\text{Mo}$ with previously published^{1,96,100} Mo data to give the systematic study desired. Other fragmentary (t,p) results are also available,^{2,3} but no study of the lighter isotopes or any attempt to give a systematic interpretation of the results had been done. In addition, there have been several (p,t) experiments⁴⁻⁶ which complement the present (t,p) study and extend the systematics to lighter nuclei. The heaviest isotopes are known from the decay of fission fragments.^{7,8} The combination of these various sets of data permits an extensive test of various models, including the unified shell-model description of nu-

clear deformation⁹ and the interacting boson approximation (IBA) model.¹⁰

II. EXPERIMENTAL TECHNIQUE

The molybdenum targets were exposed to a 17-MeV beam of tritons with an average intensity of 450 nA. The target thicknesses were between 180 and 220 $\mu\text{g}/\text{cm}^2$, and their isotopic enrichments are shown in Table I. In addition, a natural Mo target was used to establish more accurately relative cross sections among the isotopes. All of the targets were rolled, self-supporting foils. Their thicknesses were obtained from weighing as well as from the use of a monitor detector at 30° scattering angle to measure elastic scattering cross sections of the tritons. These latter results were compared with optical model calculations to obtain the target thicknesses. The optical model potential¹¹ is shown in Table II.

The reaction protons were detected in a helical cathode proportional chamber¹² in the focal plane of a quadrupole-dipole-dipole-dipole (Q3D) spectrometer.¹³ Typical resolutions were 15 keV (FWHM). Data were obtained at 11 angles in the range 10° (or 12°) to 60° with total integrated beam currents of 0.3–1.2 mC (= milli-Coulombs). The one meter long detector encompassed a 15% bite in energy, which corresponded to a 3.5-MeV range in excitation energy. Two overlapping energy bites

TABLE I. Isotopic enrichments and Q values. Percent enrichment^a in isotopes shown below.

Target	⁹² Mo	⁹⁴ Mo	⁹⁵ Mo	⁹⁶ Mo	⁹⁷ Mo	⁹⁸ Mo	¹⁰⁰ Mo	Q_m^b (keV)
⁹² Mo	97.6	0.74	0.46	0.34	0.15	0.44	0.29	9266±6
⁹⁴ Mo	0.87	93.9	2.85	1.04	0.40	0.75	0.22	8044±5
⁹⁷ Mo	0.27	0.24	0.68	1.69	92.8	3.97	0.37	6086±4
⁹⁸ Mo	0.31	0.23	0.49	0.61	0.77	97.01	0.59	5735±7

^aWe are indebted to the Stable Isotopes Division of ORNL for the enriched isotopes.

^bCalculated for the (t,p) reaction on isotope shown in column 1 by using the masses derived by A. H. Wapstra and K. Bos, *At. Data Nucl. Data Tables* **19**, 177 (1975).

were taken for those targets where excitation energies up to 5 MeV are quoted. The focal plane was calibrated using the well known excitation energies of the low-lying states of ^{94,96,99,100}Mo.

III. EXPERIMENTAL RESULTS

A. The ⁹²Mo(t,p)⁹⁴Mo results

The states populated in ⁹⁴Mo are summarized in Table III and Fig. 1 shows the spectrum at 35°. The angular distributions are seen in Fig. 2. The agreement between our results and those reported previously is generally very good. It should be noted, however, that:

(1) Since unnatural parity states cannot be excited in the (t,p) reaction by a simple direct process, the intensity of the corresponding proton groups should be very small. Many of the groups in Table III which were previously observed but which we did not populate, had been given unnatural parity assignments. Some other groups, i.e., ⁹⁴Mo(2.74, 2.93, 2.96, 3.08, 3.13 MeV) whose J^π have not been definitely assigned, are not populated in the (t,p) reaction; these may also be unnatural parity states.

(2) Some known states of ⁹⁴Mo are too closely spaced to be resolved in this (t,p) work. This is,

for instance, the case for ⁹⁴Mo(2.870, 2.872 MeV). Group 13, which corresponds to an excitation energy of 2872 keV, is too broad to be due to a single state, but its angular distribution is in good agreement with an $L=2$ shape, and therefore, the $6^{(+)}$ state does not appear to contribute substantially to its intensity. At higher excitation energies the density of states increases, and it becomes more difficult to associate the proton groups (i.e., groups 22 and 24) with known states in ⁹⁴Mo. Although the $L=0$ angular distribution is striking and can usually be readily identified, there is no indication that the previously identified 0^+ states ⁹⁴Mo(3.308 and 3.700 MeV) are populated in the present study.

(3) Some of the proton groups observed in this study have widths which are too large to be accounted for by a single state. Some of these broad groups (e.g., groups 25, 26, 29, 30, and 32) occur in regions where only single states have been previously reported, suggesting that higher resolution studies are necessary.

Furthermore, we report 18 additional states of ⁹⁴Mo with $3200 < E_x < 5060$ keV, and we report 17 determinations of J^π which had not previously been made. One of the new states [⁹⁴Mo*(3.204); $J^\pi=4^+$] is one of the most strongly populated (group 16) in this reaction.

TABLE II. Optical model parameters used in DW calculations.^a

Particle	V (MeV)	r_r (fm)	a_r (fm)	W (MeV)	W_D (MeV)	r_w (fm)	a_w (fm)	V_{so} (MeV)	r_{so} (fm)	a_{so} (fm)
t	166.7	1.16	0.752	17.1	0	1.498	0.817	6.0	1.10	0.83
p	57.2	1.17	0.75	2.6	8.0	1.32	0.51	6.2	1.01	0.75

^aTriton parameters are from Ref. 11; proton parameters from Ref. 15.

TABLE III. Energy levels of ⁹⁴Mo.

Group no. ^a	<i>E_x</i>	Present work		<i>ε</i> ^c	Previous results ^b	
		<i>L</i>	<i>J^π</i>		<i>E_x</i>	<i>J^π</i>
0	0	0	0 ⁺	1.05	0	0 ⁺
1	870±5	2	2 ⁺	1.14	871.0	2 ⁺
2	1573±5	4	4 ⁺	0.88	1573.7	4 ⁺
3	1742±5	0	0 ⁺	0.06	1742	0 ⁺
4	1864±5	2	2 ⁺	0.11	1864.2	2 ⁺
5	2068±5	2	2 ⁺	0.58	2067.4	2 ⁺
6	2294±5	4	4 ⁺	0.07	2294	(4) ⁺
7	2391±8	2	2 ⁺	0.01	2393	2 ⁺
8	2422±5	6	6 ⁺	8.7	2423	6 ⁺
9	2532±8	3	3 ⁻	0.54	2533.7	3 ⁻
10	2564±8	4	4 ⁺	0.21	2567	4 ⁺
11	2608±8				2610	(5) ⁻
					2740	
12	2772±12 ^d	4	4 ⁺	0.14	2768	π = +
					2806 ^h	(3) ⁺
					2837 ^h	(4) ⁻
13	2872±12 ^d	2	2 ⁺	0.36	2870	
					2872 ^e	6 ⁽⁺⁾
					2930	
					2055	8 ⁽⁺⁾
					2965 ^h	(3) ⁺
14	3014±12	3	3 ⁻	0.35	3012	(3) ⁺
					3026 ^h	(4) ⁻
					3083	
					3132	
15	3170±12 ^e	6	6 ⁺	5.5	3171	(3) ⁺
16	3204±10	4	4 ⁺	0.27		
17	3267±12	1	1 ⁻	0.016	3264	
					3308	0 ⁺
18	3320±20 ^e	(g)			3320	
19	3340±15 ^e				3359	(8) ⁺
					3366	(7) ⁻
20	3380±20 ^e				3375	
21	3392±15 ^d	(f)			3401	(2) ⁺
					3450	
22	3452±10	2,3	2 ⁺ , 3 ⁻		3462	
23	3534±10	2	2 ⁺	0.53	3519	
24	3620±12 ^d	(5)	(5) ⁻	(0.04)	3602	
					3650	
25&26	3714±10 ^d	(f)	(g)		3700	0 ⁺
27	3790±12	2	2 ⁺	0.11	3800	(3) ⁻
					3805	
28	3845±12	4	4 ⁺	0.16		
29	3895±12 ^d	(f)			3896	10 ⁽⁺⁾
30	3984±12 ^d	2	2 ⁺	0.41	3995	(2) ⁺
31	4032±10	5	5 ⁻	0.17	4007	
32	4079±12 ^d	4	4 ⁺	0.30	4095	(2) ⁺
33	4120±12	2,3	2 ⁺ , 3 ⁻		4140	(2) ⁺
34	4174±12	6	6 ⁺	3.9	4189	
35	4223±12	4	4 ⁺	0.087		
36	4293±12 ^e					
37	4319±15 ^e					

TABLE III. (*Continued.*)

Group no. ^a	E_x	Present work			Previous results ^b	
		L	J^π	ϵ_c	E_x	J^π
38,39	$4388 \pm 15^{d,e}$	(f)				
40	4436 ± 12	(f)				
41	4475 ± 12	(2)	(2 ⁺)	(0.14)	4495	
42	4565 ± 12^d					
43	4599 ± 12					
44	4636 ± 12^d					
45	4729 ± 15					
46	4755 ± 12					
47	4804 ± 12	(f)				
48	4833 ± 12^e					
49	4886 ± 12	(f)				
50	4921 ± 12					
51	4975 ± 12					
52	5059 ± 15					

^aSee Figs. 1 and 2.^bReference 26.^cEnhancement factor; defined in Eq. (1).^dThe group is broad and presumably corresponds to unresolved states.^eThe group is only partly resolved.^fAngular distribution of this proton group shows that it corresponds to more than one state.^gThere is no indication of a 0⁺ state in this unresolved group.^hUnnatural parity states would not contribute intense groups.

B. The ⁹⁴Mo(*t,p*)⁹⁶Mo results

The states populated in ⁹⁶Mo are summarized in Table IV, with Fig. 3 giving the spectrum at 40° and Fig. 4 the angular distributions (see also subsection A). Because of the relatively low enrichment of the ⁹⁴Mo target (93.8%), groups are observed which can be identified with known states in ⁹⁷Mo reached via the ⁹⁵Mo(*t,p*) reaction (⁹⁵Mo was present as a 2.85% component). Only the groups which could not be identified as states in ⁹⁷Mo have been given numbers identifying them as states of ⁹⁶Mo. Groups 3 and 4, which correspond to known states of ⁹⁶Mo, may also include some contributions from ⁹⁷Mo(0.89, 1.09 + 1.12 MeV), but the contributions do not appear to be important. At higher excitation energies the states in ⁹⁷Mo become poorly known, and we arbitrarily decided not to study weak groups, although in some cases (see Table IV) states of ⁹⁶Mo are known to exist at corresponding energies. At still higher excitation energies (above $E_x = 4$ MeV) we have chosen not to analyze rather strong groups (i.e., at channels 242, 203, etc.), when the E_x and the line shapes were found to vary greatly from one angle

to another. It is clear that above $E_x = 4$ MeV, the density of states in ⁹⁶Mo is such as to preclude a meaningful study with our resolution (~ 15 keV FWHM). The groups corresponding to the higher states listed in Table IV generally display angular distributions amenable to distorted wave (DW) analysis.

The agreement between our results and those reported previously is generally very good, subject to the caveats discussed in subsection A. The previously identified states ⁹⁶Mo*(2.096, 2.219, 2.441, 2.594) [$J^\pi = (2^+), (4^+), 6^+, (3,4)^+$] were in regions of the spectra, where they should have been observed had they been populated with an intensity comparable to those of nearby groups. We see no evidence for them above the level of weak structures which can be accounted for by known states of ⁹⁷Mo. The 6⁺ state at 2.441 MeV might possibly have been missed in the tail of group 8; however, the angular distribution to that group (see Fig. 4) does not show an $L = 6$ contribution. Group 11 should correspond to the unresolved states ⁹⁶Mo*(2.750, 2.755) [$J^\pi = 0^+, (6^+)$]. We observe an angular distribution which is in reasonable agreement with $L = 5$, although an optimum mix-

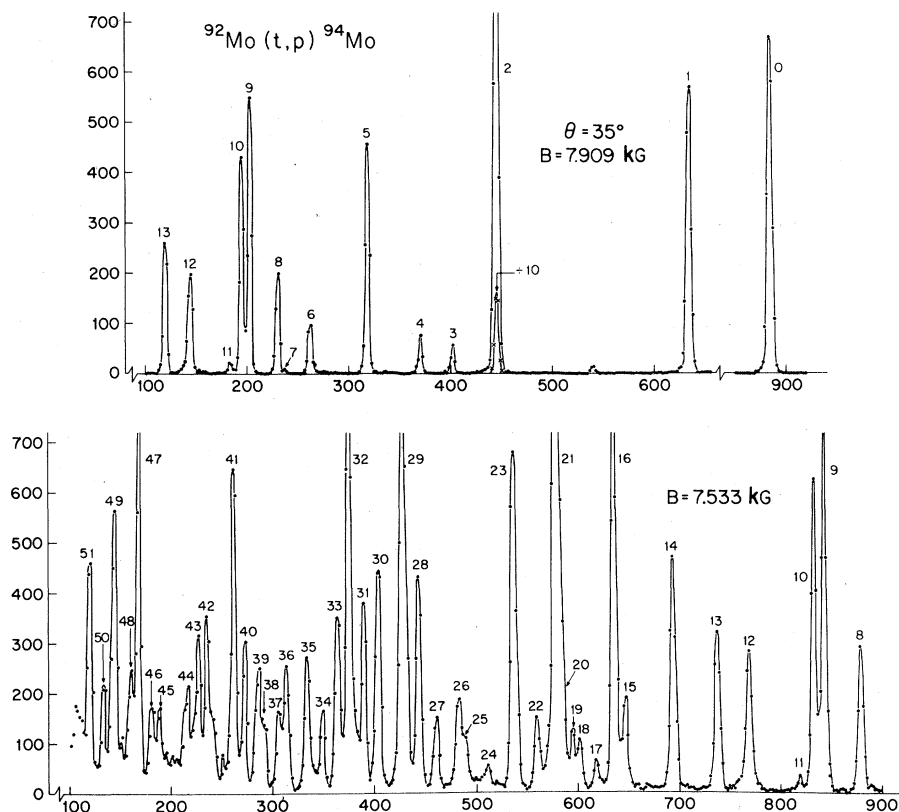


FIG. 1. Spectra of the $^{92}\text{Mo}(t,p)^{94}\text{Mo}$ reaction at 35° . The ordinate is the total number of counts in a two-channel bin. The peak numbers refer to states in ^{94}Mo ; see Table III. Unnumbered peaks are due to other Mo isotopes or to contaminants.

ture of strengths of a 0^+ and a 6^+ state might appear to yield an $L=5$ distribution. Groups 19 and 22 have angular distributions consistent with $L=2$ (and $J^\pi=2^+$) and certainly not with the previously assigned $J^\pi=(8^+)$ and (7^-) . Either those assignments are in error or we are populating different states. Further, we report 16 additional states of ^{96}Mo with $2870 < E_x < 4720$ keV, and we have made 18 new J^π assignments.

C. The $^{97}\text{Mo}(t,p)^{99}\text{Mo}$ results

The states populated in ^{99}Mo are summarized in Table V with Fig. 5 giving the spectrum at 45° and Fig. 6 the angular distributions (see also subsection A). Because of the low enrichment of ^{97}Mo (92.8%), proton groups are observed which are due to known states in ^{100}Mo [from $^{98}\text{Mo}(t,p)^{100}\text{Mo}$; see Fig. 7]; such groups are unnumbered in Fig. 5. Group 3 occurs at the location where the ground

state of ^{100}Mo would be expected. The angular distribution of group 3 (see Fig. 6), $^{99}\text{Mo}(0.351$ MeV), is consistent with $L=0+2$, suggesting the unresolved admixture of the two states.

$L=0$ transfer can only populate a $\frac{5}{2}^+$ state in ^{99}Mo . $L=2$ transfer, in principle, can populate states with $J^\pi=(\frac{1}{2} \rightarrow \frac{9}{2})^+$ (but $\frac{5}{2}^+$ could also be reached by $L=0$). $L=4$ transfer can populate states with $(\frac{1}{2} \rightarrow \frac{13}{2})^+$.

Once again agreement with previous results is satisfactory (but see subsection A). The unresolved group 8 is characterized by an E_x and an angular distribution consistent with the excitation of $^{99}\text{Mo}(0.698$ MeV); the contribution of $^{96}\text{Mo}(0.684$ MeV), which should be populated through $L=3$ transfer, does not appear to be appreciable.

$^{99}\text{Mo}(1.89, 1.91$ MeV) should also be populated by $L=3$ transfer, but while such transfers have been observed in the other Mo isotopes, groups 32 and 33 do not show the shapes characteristic of $L=3$.

Altogether we observe three $L=0$ transitions to

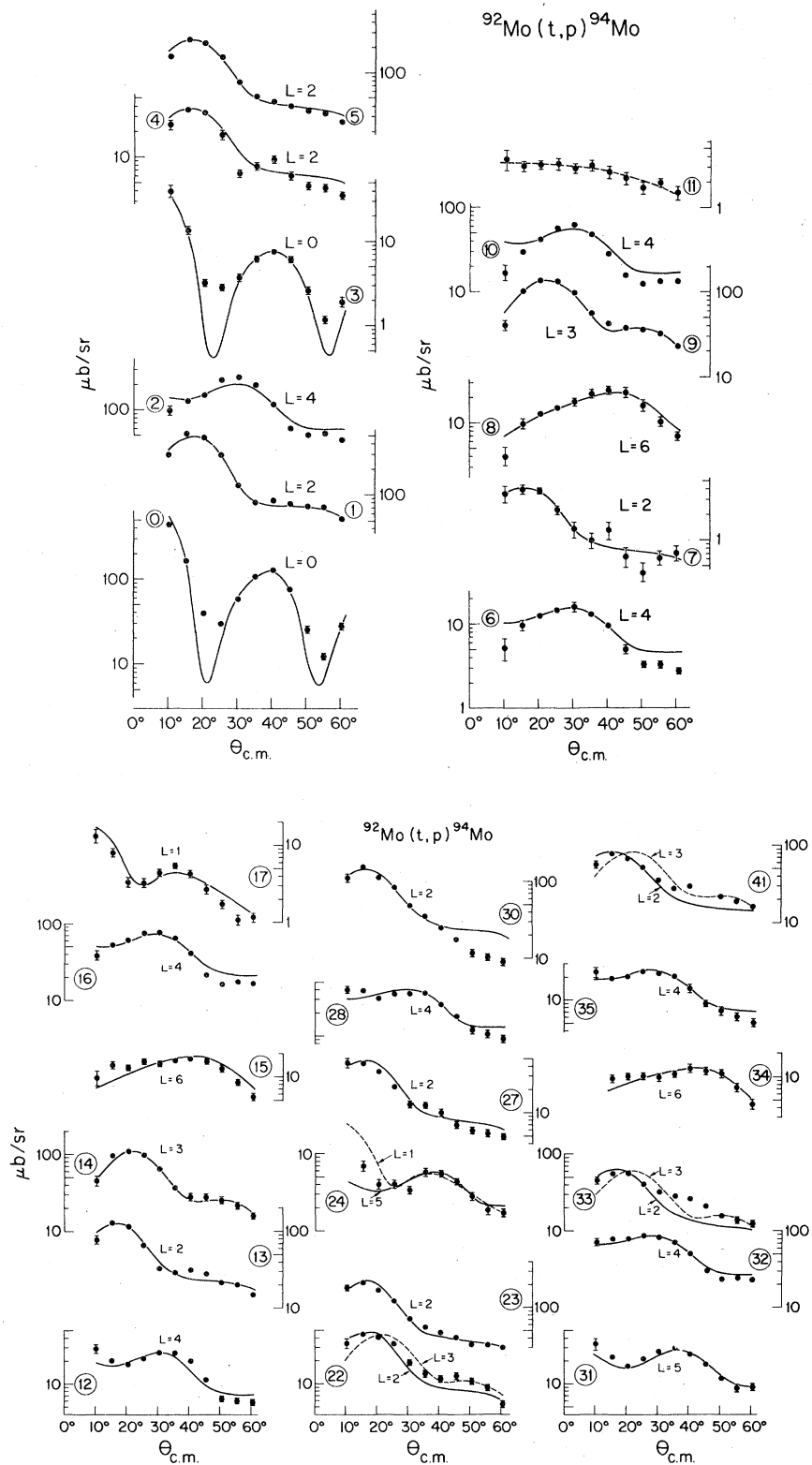


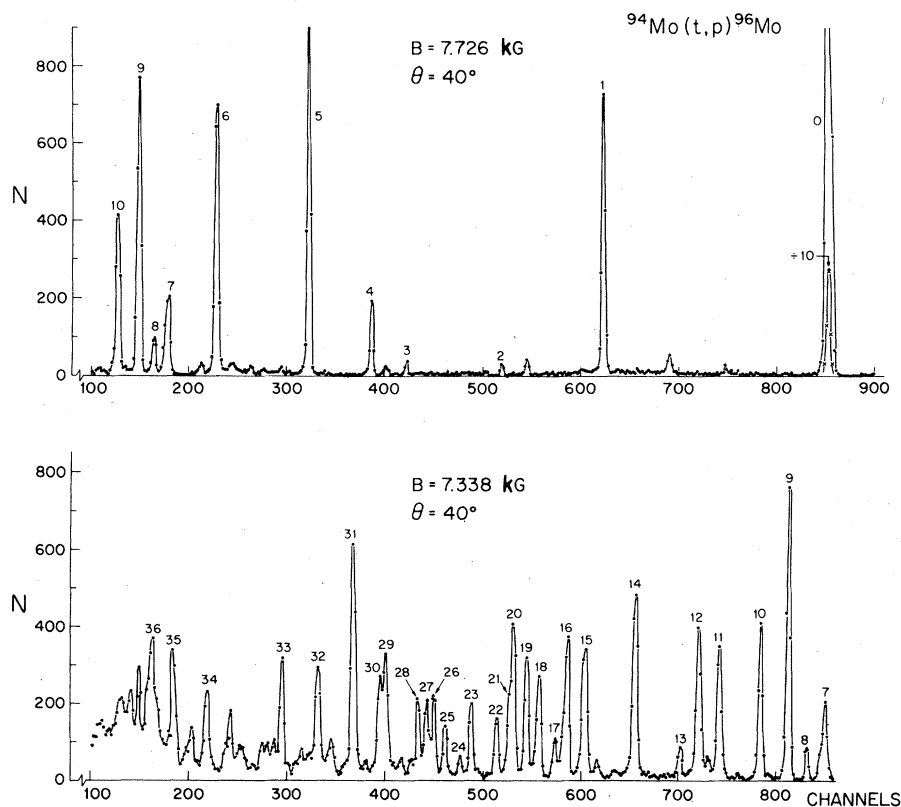
FIG. 2. Angular distributions of proton groups corresponding to ^{94}Mo states identified in Table III. The solid lines are the results of DW calculations using the parameters shown in Table II. Data points connected by dashed lines without L identification could not be fitted by the calculations.

TABLE IV. Energy levels of ⁹⁶Mo.

Group no. ^a	E_x	Present work			Previous results ^b	
		L	J^π	ϵ^c	E_x	J^π
0	0	0	0 ⁺	1.69	0	0 ⁺
1	777±3	2	2 ⁺	0.73	778.2	2 ⁺
2	1146±5	0	0 ⁺	0.02	1147.9	0 ⁺
3	1497±8	2	2 ⁺	0.03	1497.8	2 ⁺
					1625.9	2 ⁺
4	1626±5	2+4	2 ⁺ +4 ⁺		1628.2	4 ⁺
5	1866±8	4	4 ⁺	0.45	1869.5	4 ⁺
					1978.3	3 ⁺
					2095.6	(2 ⁺)
					2219.3	(4 ⁺)
6	2228±8	3	3 ⁻	1.61	2234.5	3 ⁻
7	2421±8	2	2 ⁺	0.28	2426.2	2,3,4 ⁺
					2438.3	(5 ⁺)
					2440.7	6 ⁺
8	2476±8	4	4 ⁺	0.06	2481.1	(4 ⁺)
9	2536±10	2	2 ⁺	0.77	2540.4	
					2594.5	(3,4) ⁺
10	2621±10	4	4 ⁺	0.26	2624.5	(4 ⁺)
					2700	
					2734.5	(5 ⁻)
					2750	0 ⁺
11	2755±10 ^{d,e}	(5)	(5 ⁻)	(0.07)	2754.6	(6 ⁺)
					2786.9	
					2790.2	
12	2819±10	4	4 ⁺	0.26	2818.5	
13	2875±10 ^f	(g)				
					2975.2	
					2979	6 ⁺
					2986.8	
14	3020±10	5	5 ⁻	0.11	3024.6	
					3053.2	(4 ⁺)
					3087.2	
					3133.8	
					3179	
15	3184±10 ^d	4	4 ⁺	0.26	3187	(4 ⁺)
					3203	
16	3241±12	4	4 ⁺	0.26		
17	3281±12	2	2 ⁺	0.13	3284	
18	3335±10	4	4 ⁺	0.16	3335	
19	3375±10	2	2 ⁺	0.32	3370	(8 ⁺)
20	3418±12	5	5 ⁻	0.07	3417	
21	3434±12 ^h	4	4 ⁺	0.10	3442	(2 ⁻)
22	3473±10	(2)	(2 ⁺)	(0.18)	3473	(7 ⁻)
23	3556±10	5	5 ⁺	0.03	3551	(3,4 ⁻)
24	(3593±12) ^f					
25	3646±10	(g)				
26	3683±12	(g)				
27	3709±12	2	2 ⁺	0.21		
28	3737±12	4	4 ⁺	0.12		
					3787	(10 ⁺)

TABLE IV. (Continued.)

Group no. ^a	E_x	Present work L	J^π	ϵ^c	Previous results E_x	J^π
29	3847 ± 12^b					
30	3867 ± 12^b	(5)	(5 ⁻)	(0.05)	3916	
31	3959 ± 12					
32	4080 ± 12	4	4 ⁺	0.32		
33	4205 ± 12	4	4 ⁺	0.15		
34	4471 ± 12				4533	
35	4594 ± 12				4584	
36	4714 ± 12	1	1 ⁻			

^aSee Figs. 3 and 4.^bReference 26.^cEnhancement factor, defined in Eq. (1).^dThe group is broad and presumably corresponds to unresolved states.^eNot all groups observed in the spectra are listed above this excitation energy. The reason, relating to the presence of ⁹⁵Mo(*t,p*) groups, is discussed more fully in the text (Sec. III B).^fMay be a contaminant group from ⁹⁵Mo(*t,p*)⁹⁷Mo.^gAngular distribution of this proton group shows that it corresponds to more than one state.^hThis group is only partially resolved.FIG. 3. Spectra of the ⁹⁴Mo(*t,p*)⁹⁶Mo reaction at 40°. See Table IV and the caption to Fig. 1.

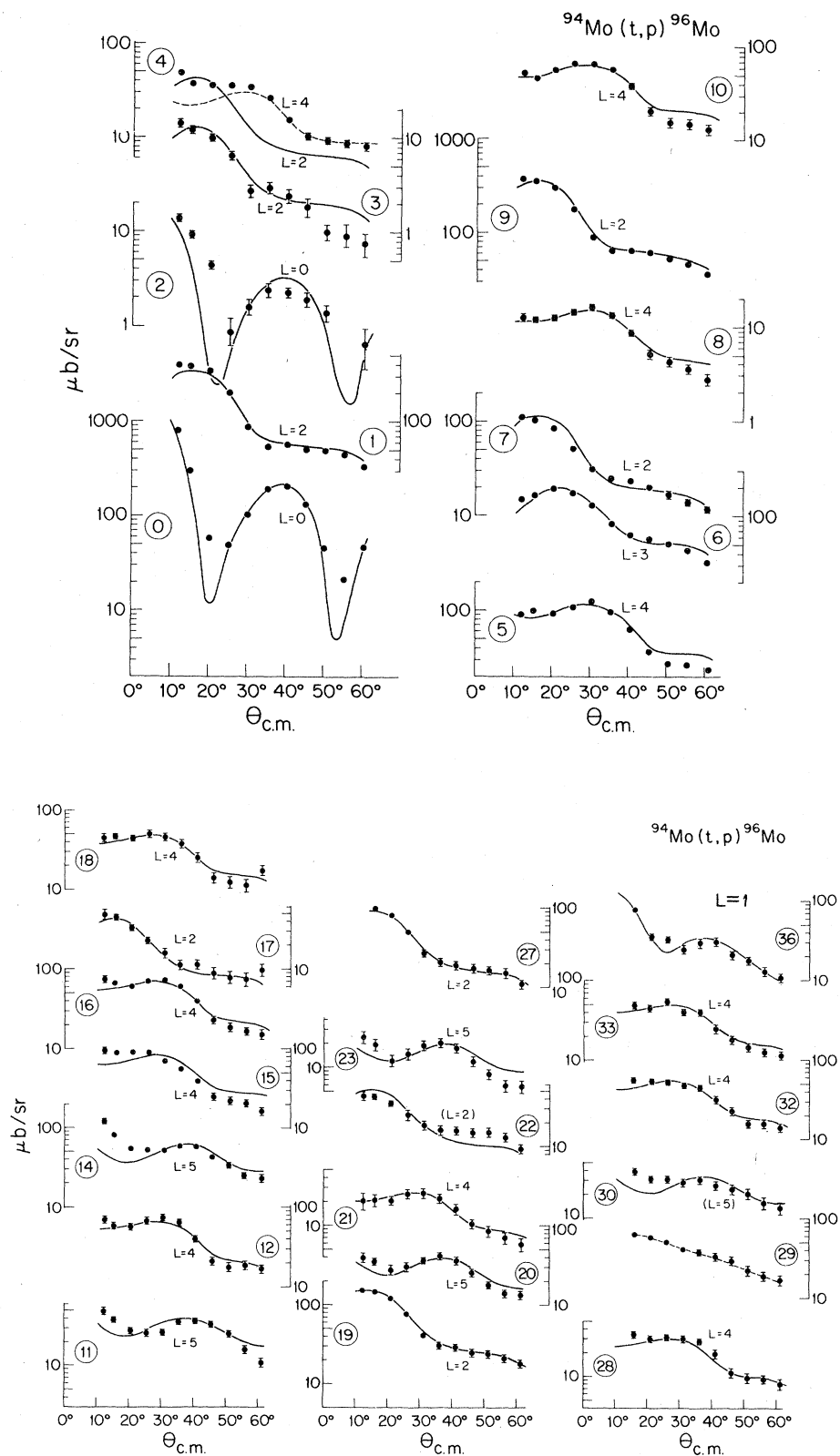


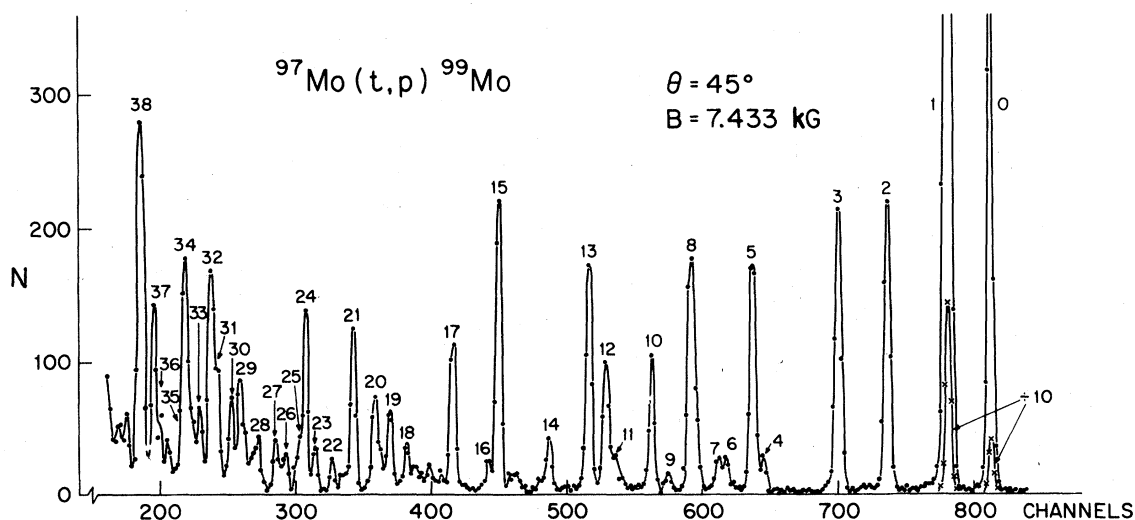
FIG. 4. Angular distributions to the ^{96}Mo states identified in Table IV. See also the caption to Fig. 2.

TABLE V. Energy levels of ^{99}Mo .

Group no. ^a	E_x (keV)	Present work			Previous results ^b	
		L	J^π ^c	ϵ ^d	E_x	J^π
0	0	2	$(\frac{1}{2} \rightarrow \frac{9}{2})^+$	0.34	0	$\frac{1}{2}^+$
1	99 ± 3	0	$\frac{5}{2}^+$	1.04	97.8	$\frac{5}{2}^+$
2	237 ± 3	4	$(\frac{7}{2} \rightarrow \frac{13}{2})^+$	0.06	235.5	$\frac{7}{2}^+$
3	352 ± 5	(e)			351.2	$\frac{3}{2}^+$
4	526 ± 5^f	2	$(\frac{1}{2} \rightarrow \frac{9}{2})^+$	0.02	525.4	$(\frac{1}{2})^+$
5	552 ± 5	4	$(\frac{3}{2} \rightarrow \frac{13}{2})^+$	0.06	548.5	$(\frac{3}{2})^+$
6	617 ± 8	2	$(\frac{1}{2} \rightarrow \frac{9}{2})^+$	0.02	615.0	$(\frac{5}{2})^+ \text{ h}$
7	635 ± 8	2	$(\frac{1}{2} \rightarrow \frac{9}{2})^+$	0.03	631.3	$(\frac{1}{2}, \frac{3}{2})^+$
					683.9	$\frac{11}{2}^-$
8	698 ± 5^g	2	$(\frac{9}{2})^+ \text{ k}$	0.18	697.9	$(\frac{5}{2}, \frac{7}{2})^+ \text{ h}$
9	753 ± 10	(i)			753.7	$(\frac{5}{2})^+ \text{ h}$
10	793 ± 5	(j)			792.4	$(\frac{3}{2})^+$
11	881 ± 10^f				889.3	$(\frac{3}{2}, \frac{5}{2})^+$
12	906 ± 8	2	$(\frac{1}{2} \rightarrow \frac{9}{2})^+$	0.07	905.5	$(\frac{1}{2})^+$
13	944 ± 5	0	$\frac{5}{2}^+$	0.10	944.4	$(\frac{3}{2}, \frac{5}{2})^+$
					1025.4	$(\frac{1}{2}, \frac{3}{2})^+$
14	1042 ± 8^g	(e)			1047	$\pi = +$
15	1164 ± 8	0	$\frac{5}{2}^+$	0.16	1166	$(\frac{3}{2}, \frac{5}{2})^+$
16	1193 ± 10^f	(e)			1200	
					1254	$(\frac{1}{2})^+$
17	1276 ± 10^g	(d)			1280	
					1353	
18	1393 ± 10	(e)			1390	$(\frac{3}{2}, \frac{5}{2})^+$
19	1432 ± 8	2	$(\frac{1}{2} \rightarrow \frac{9}{2})^+$	0.06	1442	$(\frac{3}{2}, \frac{5}{2})^+$
20	1468 ± 8^g	2	$(\frac{1}{2} \rightarrow \frac{9}{2})^+$	0.08	1466	
21	1523 ± 8^g	4	$(\frac{3}{2} \rightarrow \frac{13}{2})^+$	0.03		
					1550	$(\frac{3}{2}, \frac{5}{2})^+$
22	1575 ± 10	4	$(\frac{3}{2} \rightarrow \frac{13}{2})^+$	0.007	1570	
23	1618 ± 10	(l)				
24	1645 ± 8	4	$(\frac{3}{2} \rightarrow \frac{13}{2})^+$	0.03	1637 ± 12	$(\frac{11}{2})^- \text{ k}$
25	1661 ± 15^g				1672 ± 5	
26	1694 ± 10					
27	1721 ± 10				1722 ± 5	$(\frac{1}{2}, \frac{3}{2})^-$
28	1763 ± 15^g				1755 ± 5	$(\frac{3}{2}, \frac{5}{2})^+$
29	1804 ± 10^g				1812 ± 5	
30	1828 ± 10	2	$(\frac{1}{2} \rightarrow \frac{9}{2})^+$	0.05		
					1845 ± 5	
31	1865 ± 10^f					

TABLE V. (Continued.)

Group no. ^a	E_x (keV)	Present work			Previous results ^b	
		L	J^π ^c	ϵ ^d	E_x	J^π
32	1881 ± 10	(j)			1891 ± 15	$\frac{1}{2} - k$
33	1909 ± 10				1910 ± 20	$\frac{1}{2} - k$
34	1930 ± 10	2	$(\frac{1}{2} \rightarrow \frac{9}{2})^+$	0.04	1930 ± 5	$\frac{9}{2} + k$
35	1948 ± 15^f				1948 ± 5	$\frac{1}{2}^+$
					1965 ± 5	$\frac{1}{2}^+$
36	2000 ± 15^f					
37	2024 ± 15	1	$(\frac{3}{2} \rightarrow \frac{7}{2})^-$	0.04		
38	2059 ± 15	1	$(\frac{3}{2} \rightarrow \frac{7}{2})^-$	0.08		

^aSee Figs. 5 and 6.^bSee footnote b in Table III; L. R. Medsker, Nucl. Data Sheets **12**, 431 (1974) and P. K. Bindal, D. H. Youngblood, R. L. Kozub, and P. H. Hoffman-Pinther, Phys. Rev. C **12**, 1826 (1975).^cSee discussion in subsection III C.^dSee footnote (c) in Table III.^eThe angular distribution of this proton group shows that it corresponds to more than one state.^fThe group is only partly resolved.^gThe group is broad and presumably corresponds to unresolved states.^hThis group is very weak at all angles.ⁱThe angular distribution of this group (see Fig. 6) cannot be fitted by DW.^jAssignment from Bindal *et al.* (see footnote b, above).^kSee the text for this assignment.FIG. 5. Spectrum of the $^{97}\text{Mo}(t,p)^{99}\text{Mo}$ reaction at 45° . See Table V and the caption to Fig. 1.

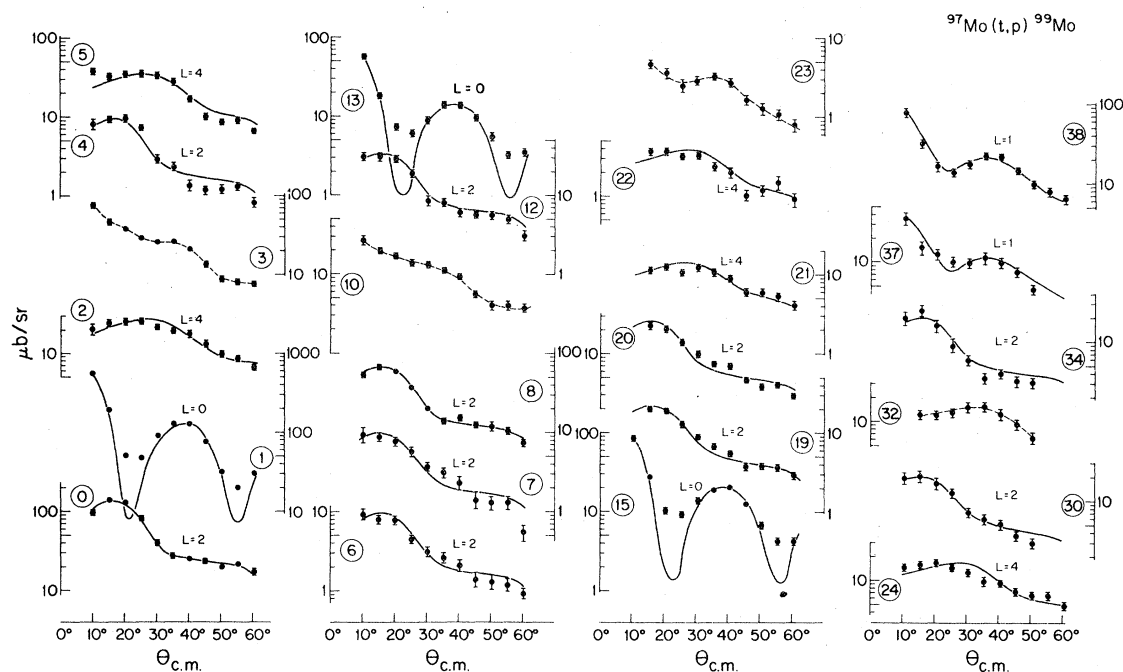


FIG. 6. Angular distributions to the ^{99}Mo states identified in Table V. See also the caption to Fig. 2.

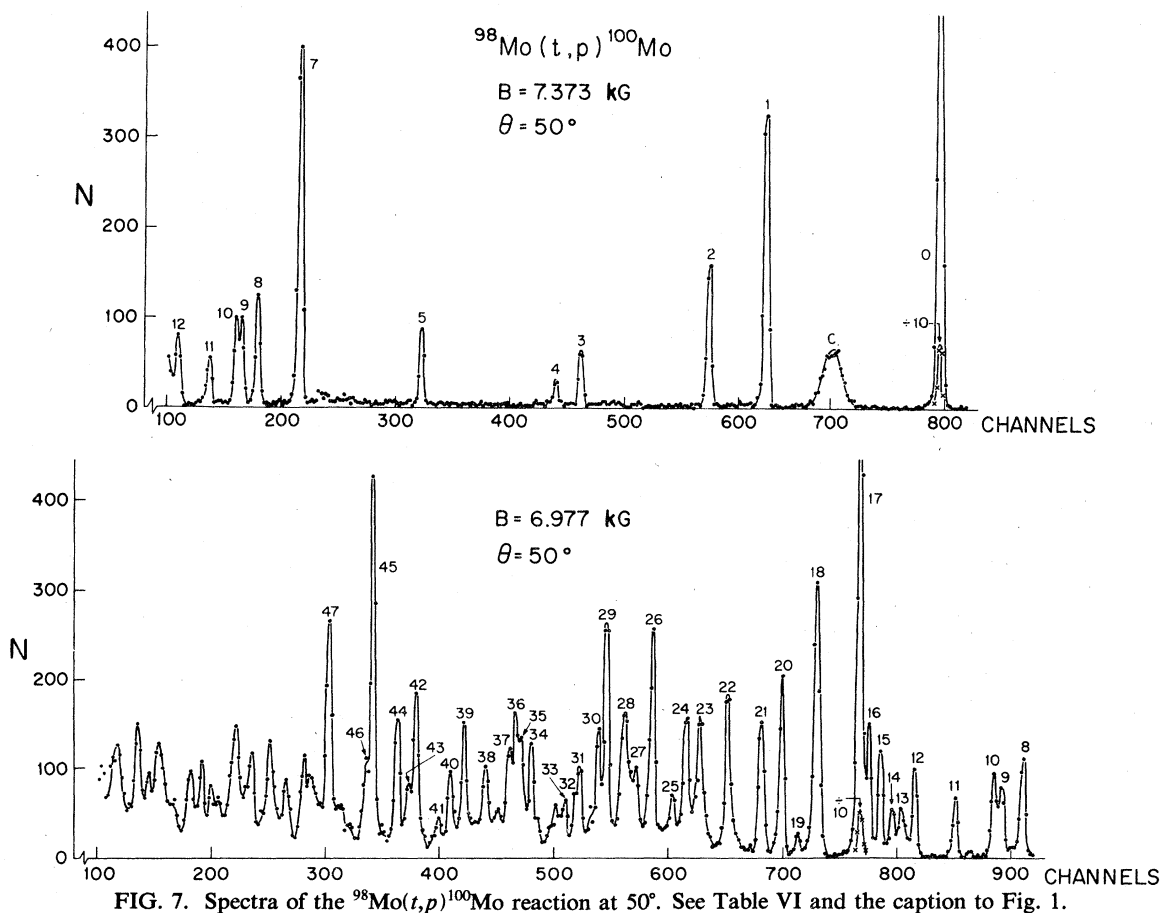


FIG. 7. Spectra of the $^{98}\text{Mo}(t,p)^{100}\text{Mo}$ reaction at 50° . See Table VI and the caption to Fig. 1.

$\frac{5}{2}^+$ states in ⁹⁹Mo at 99, 944, and 1164 keV, only the first of which had been assigned. We do not observe in this reaction (in contrast to the even-mass target measurements), *L* = 3, 5, and 6 transfers, which would tend to occur at higher excitation energies. We decided not to probe higher *E_x* states because of the increased density of states for ⁹⁹Mo, an even-odd nucleus. Further we report six new states of ⁹⁹Mo with $1.62 < E_x < 2.06$ MeV. In a number of cases our *L* determinations add additional information on the possible *J^π* of ⁹⁹Mo states. One interesting feature is the large number of states described by a single *L* transfer, even though *L* mixtures are allowed. This feature is characteristic of a particle-vibration weak-coupling structure, where the transfer in the odd-mass nucleus is characteristic of the transfer to the corresponding vibration in the even-even core.

D. The ⁹⁸Mo(*t*,*p*)¹⁰⁰Mo results

The states populated in ¹⁰⁰Mo are summarized in Table VI, with Fig. 7 giving the spectrum at 50° and Fig. 8 the angular distributions. As in the other reactions our results are in good agreement with those determined earlier (see also subsection A). We have made no attempts to identify all the proton groups which would correspond to *E_x* > 3.7 MeV in ¹⁰⁰Mo: the density of states is such as to preclude meaningful results. Of particular note in the spectrum of Fig. 7 is the strength of the 0⁺ state at 694 keV, which is 10 times the strength of the first excited 0⁺ state of ⁹⁴Mo given in Table IV. This is in contrast to the 2⁺ transition strength which has dropped a factor of 3 and the 4₁⁺ strength which has dropped a factor of ~20.

E. Levels in ⁹⁸Mo and ¹⁰²Mo

The ⁹⁶Mo(\vec{t} ,*p*)⁹⁸Mo and ¹⁰⁰Mo(\vec{t} ,*p*)¹⁰²Mo reactions have recently been studied and reported in Ref. 1. We present in Tables VII and VIII a more complete set of data from the measurements of Ref. 1, including ϵ values for transitions not reported in the earlier publication.

IV. DISTORTED WAVE ANALYSIS

The present Mo(*t*,*p*) data were compared with distorted wave (DW) analyses using the computer code DWUCK4.¹⁴ Optical model parameters as

summarized in Table II were based on a systematic study of triton¹¹ and proton¹⁵ elastic scattering. The resulting DW predictions are shown in the angular distributions in Figs. 2, 4, 6, and 8. From these results the two-nucleon spectroscopic factors ϵ were obtained using the relation

$$(d\sigma/d\Omega)_{\text{expt}} = 9.7\epsilon N (d\sigma/d\Omega)_{\text{DW}}, \quad (1)$$

where (*dσ/dΩ*) are the experimental and DW calculated cross sections, and *N* is an empirical normalization factor¹⁶ taken here as equal to 22. The calculations were done at 1 MeV excitation energy intervals, and the resulting ϵ values quoted in Tables III–VIII thus represent energy-mass independent quantities for the purpose of relating transition strengths. Primarily (*d_{5/2}*)_{0,2,4}², (*g_{7/2}*)₆², and (*d_{5/2}**h_{11/2}*)_{3-,5-,7-} configurations were used to calculate the DWUCK form factors and determining the ϵ values in Tables III–VIII.

In a pairing or shell-model formalism, more complex form factors can be constructed from the two-particle coefficients of fractional parentage or the occupation numbers. These latter quantities can be obtained either from theory or single particle transfer reactions. In particular, the even-even ground-state transition spectroscopic amplitudes are given by¹⁷

$$B_j = \sqrt{\Omega_j} U_j^A V_j^B, \quad (2)$$

where *j* is the spin of the transferred orbital, *U_j^A* and *V_j^B* are the emptiness and fullness of the target (*A*) and final nucleus (*B*), respectively, and $\Omega_j = j + \frac{1}{2}$ is the degeneracy of the orbital. For the (*t*,*p*) reaction on an odd-mass target, the *j_A* = *j_B* transition with *L* = 0 is given by¹⁷

$$B_j = (-)^l \left[\sqrt{\Omega_j} - \frac{\sqrt{2}}{2j+1} \right] U_j^A V_j^B, \quad (3)$$

which for $j = \frac{5}{2}$, *l* = 2 becomes

$$B_{5/2} = 0.864 U_{5/2}^A V_{5/2}^B \sqrt{\Omega_{5/2}}. \quad (4)$$

For *j* ≠ 5/2 the same spectroscopic amplitudes as in relation (2) are obtained.

Calculations for ground-state transitions were performed using neutron pickup reaction results^{18,19} and the relations¹⁷

$$V_j^2 = \left[\frac{1}{2j+1} \right] \sum S_j^{(i)}; \quad U_j^2 + V_j^2 = 1, \quad (5)$$

where *S_j* is the spectroscopic amplitude and the sum is over all levels (*i*) of the same *j*. The values

TABLE VI. Energy levels of ^{100}Mo .

Group no. ^a	E_x (keV)	Present work			Previous results ^b	
		L	J^π	ϵ^c	E_x	J^π
0	0	0	0^+	1.41	0	0^+
1	535 ± 5	2	2^+	0.22	535.6	2^+
2	694 ± 5	0	0^+	0.20	694.4	0^+
3	1063 ± 5	2	2^+	0.03	1063.7	2^+
4	1136 ± 5	4	4^+	0.02	1136.1	4^+
5	1464 ± 5	2	2^+	0.05	1463.3	(2^+)
6	1502 ± 8^d	0^d	0^+	0.013	1503	
					1765.7	
		(e)				
					1770.4	
7	1907 ± 5	3,4	$3^-, 4^+$		1908.1	3^-
		(f)			(1976)	
8	2035 ± 10	0	0^+	0.09	2033	0^+
9	2082 ± 10	1	1^-	0.025	2085.6	
10	2102 ± 10	(4)	(4^+)	(0.08)	2101.4	
11	2186 ± 15	(g)			(2200 \pm 10)	
12	2281 ± 15	2	2^+	0.06		
13	2312 ± 15	(g)				
14	2334 ± 20^h				2340 ± 10	2^+
15	2634 ± 15	3	3^-	0.04		
16	2392 ± 15	(2) ^k	(2^+)	(0.14)		
17	2413 ± 15	2,3	$2^+, 3^-$		2415.6	3^-
18	2518 ± 15^i	(g)			2470 ± 10	4^+
19	2561 ± 15^i	(g)			2563.2	
20	2602 ± 15	5,6	$5^+, 6^-$		2590 ± 10	4^+
21	2652 ± 15^i	2	2^+	0.13	2670 ± 10	
22	2733 ± 15	2	2^+	0.11	2720 ± 10	
23	2803 ± 15	(4)	(4^+)	(0.10)		
24	2835 ± 15	(4)	(4^+)	(0.08)	2830 ± 10	4^+
25	2873 ± 15					
26	2923 ± 15	(4)	(4^+)	(0.14)	2920 ± 10	5^-
27	2968 ± 15^j					
28	2994 ± 15^j					
29	3039 ± 15	4,5	$4^+, 5^-$		3030 ± 10	4^+
30	3065 ± 15	2	2^+	0.08		
31	3106 ± 20					
32	3119 ± 20^j					
33	3148 ± 15^{ij}				3150 ± 10	
34	3235 ± 15	(g)				
35	3263 ± 15^{ij}					

of V_j^2 used are given in Table IX. The resulting values of ϵ_j are given in Table X, along with the spectroscopic amplitudes.

V. DISCUSSION

A. $L=0$ transitions

The two-nucleon spectroscopic factors ϵ for ground-state transitions for the Mo nuclei are sum-

marized in Table XI. Using a simple $(d_{5/2})_0^2$ configuration for the form factor yields a widely varying value for ϵ , indicating that the configuration of the ground states is changing rapidly and/or the strong pairing correlations, as in the tin region, are not realized, which tend to give equal ϵ values for the even-even ground-state transitions. Use of mixed wave functions, as obtained from the occupation numbers of Table IX yields less fluctuation in ϵ , although it overpredicts the overall cross sec-

TABLE VI. (Continued.)

Group no. ^a	E_x (keV)	Present work			Previous results ^b	
		L	J^π	ϵ^c	E_x	J^π
36	3282 ± 2^j				3280 ± 10	
37	3306 ± 20^h					
38	3354 ± 15	2	2^+	0.08	3360	
39	3409 ± 15	(g)				
40	3445 ± 15	(g)			3440	
41	3475 ± 15	(l)				
42	3535 ± 15	(g)			3510	
43	3557 ± 15^i	2	2^+	0.04		
44	3587 ± 15	(3)	(3^-)			
45	3652 ± 15	5,6	$5^-, 6^+$		3650	
46	3674 ± 15^h				3720	
47 ^m	3771 ± 15^g	5,6	$5^-, 6^+$			

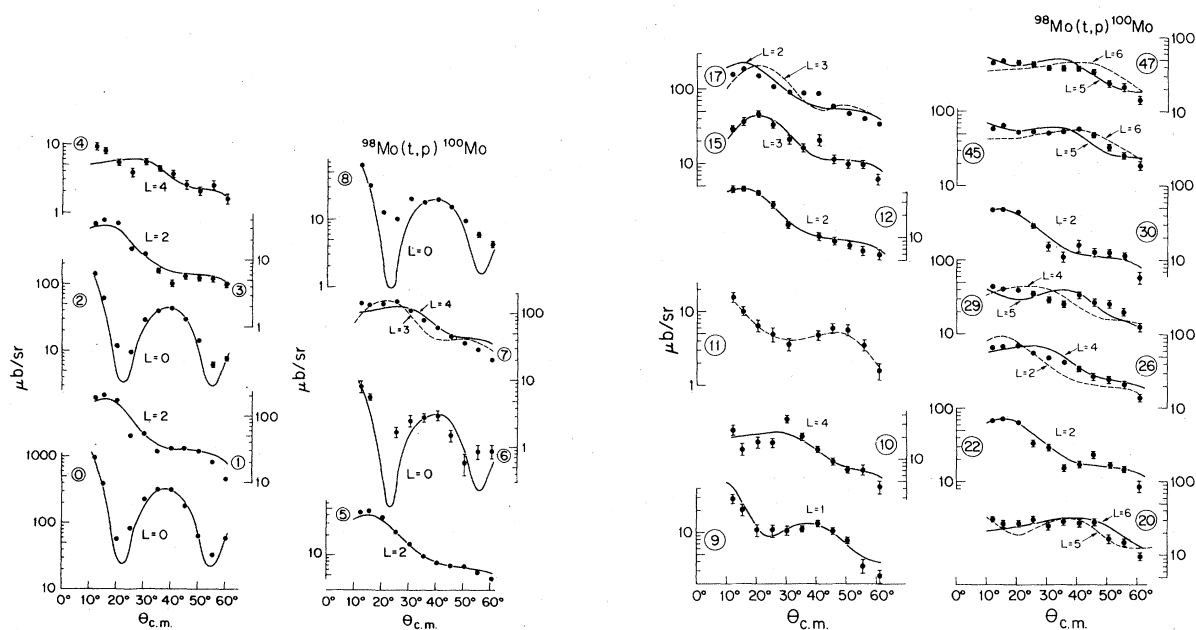
^aSee Figs. 7 and 8.^bSee footnote b in Table III and D. C. Kocher, Nucl. Data Sheets **11**, 279 (1974).^cEnhancement factor; defined in Eq. (1).^dObserved clearly at five forward angles.^eA group is observed for $\theta \leq 40^\circ$ which might be due to these two (unresolved) states. The intensity of the group is $\leq 5\%$ of the intensity of group 7 at the same angle.^fNot observed at any angle: $I \leq 2\%$ of group 7.^gThe angular distribution of this proton group cannot be analyzed using DW.^hClearly resolved only for $\theta \geq 45^\circ$.ⁱThe group is broad and presumably corresponds to unresolved states.^jThe group is only partly resolved.^kConsistent with $L = 2$; not plotted because poorly resolved at several angles.^lObserved for $25^\circ \leq \theta \leq 55^\circ$.^mGroups corresponding to higher E_x were not analyzed because of the density of states.FIG. 8. Angular distributions to the ^{100}Mo states identified in Table VI. See also the caption to Fig. 2.

TABLE VII. Energy levels of ^{98}Mo .

Group no.	Present work ^a				Previous results ^b	
	E_x (keV)	L	J^π	ϵ^c	E_x (keV)	J^π
0	0	0	0^+	1.65	0	0^+
1	735 ± 5	0	0^+	0.02	735	0^+
2	787 ± 5	2	2^+	0.52	787	2^+
3	1432 ± 5	2	2^+		1432	2^+
4	1510 ± 5	(4)	(4^+)		1510	4^+
					1758	2^+
					1812	
					(1881)	
5	1965 ± 5	0	0^+	0.05	1965	0^+
6	2018 ± 5	3	3^-	0.59	2018	3^-
					2039	
					2105	
7	2207 ± 5	2	2^+	0.20	2207	(2^+)
8	2224 ± 5	4	4^+	0.12	2224	($3, 4^+$)
9	2336 ± 5^d	(2 + 6)	($2^+ + 6^+$)	0.37(2^+)	2333	
					2344	6^+
10	2419 ± 5	2	2^+	0.05	2420	(3^-)
					2458	
					2506	
11	2530 ± 5	2	2^+	0.15	2530	
12	2573 ± 8	4	4^+	0.32	2562, 2571	
					2573	
13	2617 ± 8	0	0^+	0.16	2620	0^+

^aResults are a more complete tabulation of data originally given in Reference 1.

^bReference 26.

^cEnhancement factor defined in Eq. (1).

^dDoublet but dominated by 2333 keV state.

tions by a factor of 2. Thus, aside from the disagreement in the absolute value of ϵ , the changes in occupation numbers, as measured from single neutron pickup reaction studies, account for most of the changes in cross section for the ground-state transitions.

Of particular interest is the correction for the small value of ϵ in the odd targets which is obtained in the full wave function calculation. That the $d_{5/2}$ orbital is blocked by a factor of 0.864 [Eq. (4)], does seem to account for this reduction in section and is approximately the same for both ^{95}Mo and ^{97}Mo targets.

Examination of the ϵ values in Tables III–VIII shows a gradually decreasing value of ϵ for the even- A ground-state transitions above $A = 98$. At the same time, increasing $L = 0$ strength is seen to excited states in ^{100}Mo and ^{102}Mo . Thus, as noted in Ref. 1, there is a tendency to preserve the

overall $L = 0$ strength, or in the language of elementary excitations, the total pairing excitation is conserved. This rule is met here as well by the sum of the $L = 0$ ϵ values in ^{98}Mo , ^{100}Mo , ^{102}Mo being equal to each other to within 20%. This tendency is supported by a smooth trend in two-neutron binding energies as a function of A , which accounts for the empirical values to within 100 keV when the energy centroids of the 0^+ states are used.

B. $N = 52$ and 54

The $^{92,94}\text{Zr}$ level structure²⁰ and two-neutron transfer strengths have been well described by shell model calculations.²¹ The behavior of their isotones $^{94,96}\text{Mo}$ seems very similar and indicates that the shell model might describe the light mass Mo nu-

TABLE VIII. Energy levels of ^{102}Mo .

Group no.	Present results ^a			ϵ^c	Previous results ^b	
	E_x (keV)	L	J^π		E_x (keV)	J^π
0	0	0	0^+	1.28	0	0^+
1	296 ± 5	2	2^+	0.28	296	2^+
2	699 ± 5	0	0^+	0.60	696	0^+
					743	(4^+)
3	850 ± 5	2	2^+	0.12	850	
4	1251 ± 5	2	2^+	0.04	$1251(2^+)$	
					1305	(6^+)
5	1334 ± 5	0	0^+	0.11	1334	(0^+)
6	1881 ± 5	3	3^-	0.16	1880	
					1957	(8^+)
7	2120 ± 5				2120	
8	2239 ± 5	(4)	(4^+)		2240	
9	2321 ± 8					
10	2389 ± 8				2390	
11	2416				2420	
12	2504				2500	
13	2523				2520	
14	2545				2540	
15	2617				2620	
16	2662				2670	
17	2705	2	2^+	0.10	2700	
18	2745				2740	
19	2855				2860	
20	2875				2880	
21	2972				2970	
22	3011	2	2^+	0.52	3010	

^aResults are a more complete tabulation of data given in Reference 1.^bReference 26.^cEnhancement factor in Eq. (1).

clei as well. In particular, the 2_1^+ states in $^{94,96}\text{Mo}$ occur at essentially the same excitation energy as the 2_1^+ states in $^{92,94}\text{Zr}$, namely ~ 800 keV for Mo and ~ 900 keV for Zr. Similarly, the 4_1^+ states oc-

cur in the $N=52$ and $N=54$ nuclei at $1.5-1.7$ MeV in excitation. A comparison of ^{92}Zr with ^{94}Mo is shown in Fig. 9.

The transition strengths to the ground, 2_1^+ , and

TABLE IX. Occupation probabilities V_j^2 .

Isotope	Reference	$2d_{5/2}$	$3s_{1/2}$	Orbital $2d_{3/2}$	$1g_{7/2}$	$1h_{11/2}$
^{92}Mo		0	0	0	0	0
^{94}Mo	a	0.25	0.10	0.07	0.02	0
^{96}Mo	a	0.52	0.19	0.15	0.21	0.03
^{98}Mo	b	0.48	0.20	0.18	0.20	0.02
^{100}Mo	a	0.66	0.53	0.34	0.35	0.09

^aReference 18.^bThese values are an average of values quoted in Refs. 4 and 19.

TABLE X. Spectroscopic amplitudes and ϵ values for mixed ground-state configurations.

	$d_{5/2}$	$s_{1/2}$	B_j^a $d_{3/2}$	$g_{7/2}$	$h_{11/2}$	ϵ
$^{92}\text{Mo} \rightarrow ^{94}\text{Mo}$	0.866	0.316	0.374	0.283	0	0.45
$^{94}\text{Mo} \rightarrow ^{96}\text{Mo}$	1.082	0.414	0.528	0.907	0.424	0.44
$^{95}\text{Mo} \rightarrow ^{97}\text{Mo}$	0.746	0.347	0.606	0.817	0.541	0.42
$^{96}\text{Mo} \rightarrow ^{98}\text{Mo}$	0.831	0.402	0.553	0.795	0.341	0.65
$^{97}\text{Mo} \rightarrow ^{99}\text{Mo}$	0.74	0.347	0.606	0.817	0.541	0.42
$^{98}\text{Mo} \rightarrow ^{100}\text{Mo}$	1.015	0.651	0.747	1.058	0.727	0.46
$^{100}\text{Mo} \rightarrow ^{102}\text{Mo}$	0.790	0.346	0.600	0.820	0.542	(0.33)

^aThe B_j values were obtained using Eq. (2) and the V_j^2 values of Table IX, except for $^{95,97}\text{Mo}$ targets where an average of ^{96}Mo and ^{98}Mo V_j^2 (with $d_{5/2}$ blocked by 0.864 as indicated in the text) have been used. For $^{100}\text{Mo} \rightarrow ^{102}\text{Mo}$, an extrapolation of the V_j^2 values were used for ^{102}Mo , thus the ϵ value is only suggestive.

4_1^+ states in $^{92,94}\text{Zr}$ have been reproduced using the shell-model calculations of Ball and Bhatt.²¹ In these calculations, the ground states are mixtures of $(2d_{5/2})_0^2$, $(2d_{3/2})_0^2$, and $(3s_{1/2})_0^2$ orbitals, which are the same orbitals that dominate the structure of the $^{94,96}\text{Mo}$ isotones, as seen in Table X. Given the similar structure of the ground states of the Zr and Mo $N=52$ and $N=54$ isotones and the similarity in excitation energy for the 2_1^+ and 4_1^+ states in these nuclei, a correspondence in the microscopic structure of these low-lying excitations probably also exists. In our present measurements, the ϵ values for the 2^+ and 4^+ states in Mo were determined by assuming a simple $(d_{5/2})_{2,4}^2$ configurations for the DW form factor. Except for the 4_1^+

state in ^{96}Mo , the ϵ values given in Tables III and IV for the 2_1^+ states in $^{94,96}\text{Mo}$ and the 4_1^+ state in ^{94}Mo are approximately equal to 1.0, indicating that the $(d_{5/2})^2$ component is dominant, in agreement with the more detailed shell-model calculations for $^{92,94}\text{Zr}$, which also give good agreement with experimental strengths.²⁰ Although the 2_1^+ and 4_1^+ states in ^{94}Zr are still dominantly a $(d_{5/2})^2$ configuration, the fraction is less, and shell-model orbitals other than $(d_{5/2})^2$ are probably being reflected in the smaller ϵ value for the 4_1^+ state in ^{96}Mo .

The comparison between the $N=52$ and 54 isotones can be extended to higher excited states as well. In ^{92}Zr there are two 2^+ states, at 2071 and

TABLE XI. Two-neutron transfer strengths for ground-state transitions in $\text{Mo}(t,p)$ reactions.

Final ^a nucleus	ϵ	$(d_{5/2})^2$ Transfer ^b		Mixed transfer ^c	
		ϵ_{rel}	$(d_{5/2})^n$	ϵ	ϵ_{rel}
^{94}Mo	1.05	$\equiv 1.00$	$\equiv 1.00$	0.45	$\equiv 1.00$
^{96}Mo	1.69	1.61	1.67	0.44	0.98
^{97}Mo	0.35	0.33		0.42	0.93
^{98}Mo	1.65	1.57	1.00	0.65	1.44
^{99}Mo	0.34	0.32		0.42	0.93
^{100}Mo	1.41	1.34		0.46	1.02
^{102}Mo	1.28	1.22		0.33	0.73

^aThe results are taken from Ref. 1 ($^{98,102}\text{Mo}$) and the present study, where the ^{97}Mo result was obtained from the comparison of ground-state strengths observed with the natural Mo target.

^b ϵ values obtained using a $(d_{5/2})^2$ form factor which are compared to the predictions of a $(d_{5/2})^n$ shell model configuration.

^c ϵ values obtained using the B_j spectroscopic amplitudes of Table X.

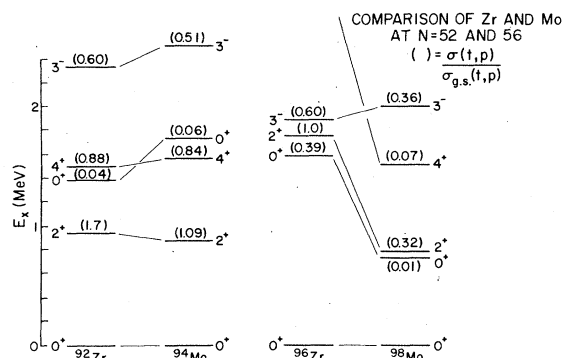


FIG. 9. Comparison of ^{92}Zr and ^{94}Mo as well as ^{96}Zr and ^{98}Mo low-lying levels.

3063 keV, which have large (t,p) transition strengths. In the shell-model calculations their dominant configuration is $(2d_{5/2}3s_{1/2})_2$, which has a large (t,p) cross section and accounts for much of the empirical strength. In ^{94}Mo two intense $L=2$ transitions populate states at 2068 and 2872 keV. It would appear likely that these two states correspond to the configurations observed at similar energies in ^{92}Zr . Although there is considerable $L=4$ transfer observed in ^{94}Mo in the 2.5–3.5 MeV energy region and although $L=4$ strength is also observed in ^{92}Zr , the lack of a complete analysis of the ^{92}Zr measurement in this energy range limits the comparison one can make.

The lowest (6^+) state in ^{92}Zr is at 2958 keV, compared to 2422 keV in ^{94}Mo . The $^{91}\text{Zr}(d,p)$ data²² indicate the 6^+ state in ^{92}Zr is dominated by the $(d_{5/2}g_{7/2})_6$ configuration. The ^{94}Mo 6^+ state is rather intensely populated in the (t,p) reaction and may be of similar configuration [the ϵ value of Table III assumes a $(g_{7/2})_6^2$ configuration].

In ^{96}Mo , 2^+ states at 2421 and 2536 keV are populated with high intensity, with the 2536 keV transition being stronger than the 2_1^+ state transition. Similar structure exists in ^{94}Zr , with strongly populated 2^+ states at 1675 and 2374 keV. In the shell-model calculations, these states in ^{94}Zr are predominantly of $(d_{5/2}s_{1/2})_2$ configuration, although these calculations only explain the empirical strengths to within a factor of 2. A comparison between the considerable $L=5$ strength in ^{96}Mo at 2.5–3.5 MeV and similar strength in ^{94}Zr is difficult because of the limited analysis of the higher-lying states in ^{94}Zr .

C. $N=56-60$

In ^{96}Zr the subshell closure of the $d_{5/2}$ orbital is attained, and the 2_1^+ state occurs much higher in the spectrum, with the 4_1^+ state lying even higher

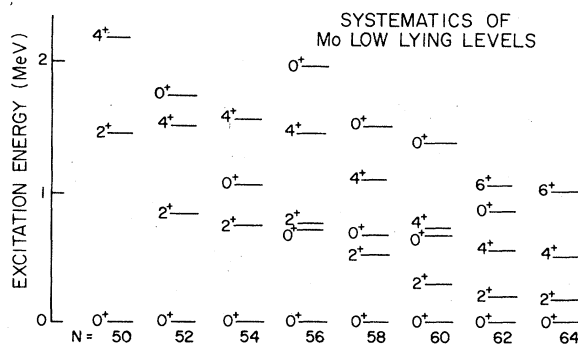


FIG. 10. Systematics of low-lying states of Mo isotopes. The data are taken from Refs. 8, 26, and the present study.

and the 4^+ strength greatly reduced²⁰ compared to $^{92,94}\text{Zr}$. This type of behavior does not occur in ^{98}Mo (see Fig. 9). Rather, as seen in Fig. 10, for ^{98}Mo the 2_1^+ state drops in energy, and the 4_1^+ state stays near 1.5 MeV, as in $^{94,96}\text{Mo}$. The low-lying 2^+ transfer strength also differs for the $N=56$ isotones; in ^{96}Zr the strength is nearly that of ^{94}Zr , while in ^{98}Mo the strength is only half that of ^{96}Mo . Both the systematics in energy and transfer strengths of the 2_1^+ states for $N=56$ indicate that, while ^{96}Zr is still following many of the trends expected from the shell model, the character of ^{98}Mo is deviating from a simple shell-model description and may be more indicative of a transitional structure towards deformation.

It is also at $N=56$ that excited $L=0$ strength starts to become important. One very interesting point is that both nuclei have a 0^+ state as their first excited state, which is an unusual occurrence in nuclei. However, these states are excited completely differently by the (t,p) reaction, indicating that they have quite different properties. The 735-keV state in ^{98}Mo has only 1.5% of the ground-state transition strength, whereas the 1594-keV state in ^{96}Zr , at twice the excitation energy of the ^{98}Mo state, contains 40% of the corresponding ground-state transition strength. The ^{96}Zr state exhibits properties similar to a pairing vibration state formed due to the strong subshell closure of the $d_{5/2}$ orbital, whereas the ^{98}Mo state has properties more similar to states in a transitional nucleus (see Ref. 1) as it is excited with 17% of the ground-state transition strength in the $^{100}\text{Mo}(p,t)^{98}\text{Mo}$ reaction.⁴ The behavior of the 2_1^+ and 0^+ state systematics indicate that an increasing trend towards deformation in the Mo isotopes washes out the subshell closure which is so dramatically illustrated in ^{96}Zr .

The heaviest Zr-Mo isotopes which can be com-

pared in the (t,p) reaction are ^{98}Zr and ^{100}Mo . The ^{98}Zr nucleus, as excited by the (t,p) reaction,²⁰ appears to be quite distinct from the lighter isotopes and again exhibits behavior expected from ^{96}Zr being a closed neutron subshell nucleus. No low-lying 0^+ states were seen, not even the 0^+ state at 850 keV reported in fission fragment decay scheme studies.⁸ In contrast, the lowest observed 0^+ state in ^{100}Mo is at 694 keV and is seen with 14% of the ground-state transition strength. Again the ^{100}Mo 2_1^+ energy follows the systematic trend towards lower excitation energies, whereas the 2_1^+ state energy of ^{98}Zr remains high at 1224 keV, 2.3 times the ^{100}Mo energy. There is very little correspondence between the two nuclei, emphasizing again the breakdown in subshell effects by the addition of two more protons.

Although their two-neutron transfer properties cannot be compared, the level spacings of ^{100}Zr and ^{102}Mo are quite similar, with the 2_1^+ state quite low in energy and a low-lying excited 0^+ state. In ^{102}Mo the 699 keV 0^+ state is populated in the (t,p) reaction with $\sim 50\%$ of the ground-state strength. These trends are indicative of a more collective, deformed structure becoming dominant, in contrast to the shell-model structure of the lighter Zr and Mo isotopes. A systematic picture of the low-lying states of the Mo isotopes is shown in Fig. 10.

The low-lying 2_1^+ state of ^{102}Mo may indicate a rotational nucleus, but the data given in Ref. 1 do not indicate a corresponding 4^+ state belonging to this band. Fission fragment decay scheme results⁸ do suggest a 4^+ state at 743 keV, which gives an energy ratio of $E_{4^+}/E_{2^+}=2.5$, somewhat below the rotational limit of 3.3. It is possible to conjecture the existence of excited deformed bands in the lighter Mo nuclei, but such ideas are highly speculative given the present knowledge of these levels. The absent or weak excitation of the 4_1^+ state in ^{102}Mo by the (t,p) reaction does correspond to behavior typical of a rotational band.

D. $L=3$ transitions

The 3_1^- states in the Mo isotopes show a gradual decrease in energy from 2533 keV in ^{94}Mo to 1881 keV in ^{102}Mo . The transition strengths to these states are characterized by $\epsilon=0.5\rightarrow 0.7$ from ^{94}Mo to ^{100}Mo , but ϵ drops significantly at ^{102}Mo to 0.16. The energy trend agrees quite well with that of octupole states in the Zr isotopes²⁰ and indicates that these octupole states are quite collective and, thus, relatively independent of subshell effects both

in Zr and Mo. The sharp drop in strength at ^{102}Mo is not completely understood, but may result from a change in deformation between target and final state.

E. Possible multiplet structure of ^{99}Mo

The (t,p) reaction on odd targets has proven to be a useful tool to study particle-vibration multiplets.²³⁻²⁵ In such cases, the spin of the target nucleus, $\frac{5}{2}^+$ for ^{97}Mo , couples to the spin of the transferred pair to produce the multiplets in the final nucleus. In the present $^{97}\text{Mo}(t,p)$ reaction, the ground-state spin of ^{99}Mo is $\frac{1}{2}^+$, so the ground state and the multiplets based on coupling of the ^{98}Mo collective core states to a $\frac{1}{2}^+$ single-particle state will not be the multiplets excited by the (t,p) reaction. Many pure L transfers are seen in this reaction indicating particle-vibration coupling is still important.

The lowest multiplet excited by the (t,p) reaction will be the $(2^+ \otimes \frac{5}{2}^+)_{1/2^+ \rightarrow 9/2^+}$. Of these states, all except the $\frac{9}{2}^+$ are able to mix easily with nearby single-particle levels, so that a pure particle vibration is not expected. The centroid of this multiplet should be around 600 keV, which is near the positions of the 2^+ states in ^{100}Mo and ^{98}Mo . This structure will be further complicated because the nature of this core state is changing from spherical to deformed. There is a group of states in the 600 keV region in ^{99}Mo , of which the strongest is the $L=2$ transfer at 698 keV. This state is not seen in (d,p) or (d,t) reactions¹⁸ and is listed in the literature²⁶ as $(\frac{5}{2}, \frac{7}{2})^+$. We suggest that it is the $\frac{9}{2}^+$ member of the $(2^+ \otimes \frac{5}{2}^+)$ multiplet. The strength should be fragmented according to $(2J_f+1)(2J_i+1)^{-1}(2L+1)^{-1}$ or, for the $\frac{9}{2}^+$ state, one third of the total strength to the 2_1^+ state in the even core. As stated above, the nature of the 2_1^+ state is changing, and the ϵ value goes from 0.52 in ^{98}Mo to 0.22 in ^{100}Mo . The value of ϵ for the 698 keV state is 0.18, which is one third of that of the ^{98}Mo 787 keV state. Other states of this multiplet are difficult to identify because of probable mixing with single-particle states. A group of $L=3$ transitions from the $(3^- \otimes \frac{5}{2}^+)_{1/2^- \rightarrow 11/2^-}$ multiplet should be seen near 2 MeV excitation energy, but none can be definitely identified.

F. IBA-2 calculations

Recently, the structure of the Ru and Pd isotopes has been successfully investigated²⁷ using the

two-boson interacting boson approximation (IBA-2) model.²⁸ In the IBA-2 model, neutron and proton bosons are treated separately and interact via a quadrupole interaction. The calculations of Ref. 27 were able to reproduce the systematics of the low-lying 2^+ and 4^+ states in Ru and Pd. The Ru nuclides are known to become rather deformed, with the 2_1^+ state dropping rapidly in energy as a function of increasing neutron number, while in Pd the 2_1^+ state energy is more constant and the shape change does not occur. The IBA-2 calculations²⁷ reproduce these differences between Ru and Pd as well.

The Hamiltonian used in Ref. 27 was of the form

$$H = \epsilon(n_{d\pi} + n_{d\nu}) + \kappa Q_\pi Q_\nu + V_{\pi\pi} + V_{\nu\nu} + M_{\pi\nu}, \quad (6)$$

where

$$Q_\pi = (d_\pi^\dagger \tilde{d}_\pi)^{(2)} + \chi_\pi (s_\pi^\dagger \tilde{d}_\pi + d_\pi^\dagger s_\pi)^{(2)} \quad (7)$$

is the quadrupole proton-neutron interaction. The V terms are interactions only between pairs of neutron bosons or pairs of proton bosons, and M is the Majorana term, taken to be constant, that pushes up the states that are not fully symmetric combinations of neutrons and protons. As noted in Ref. 27 the effects of adding $V_{\pi\pi}$ are negligible, and the $V_{\nu\nu}$ term affects only minor details of the spectra. Therefore, the important parameters are ϵ , κ , χ_π , and χ_ν . The calculations²⁷ were done for the neutron numbers 54–78. χ_ν will be the same for a series of isotones and χ_π will be the same for a series of isotopes, so that only ϵ and κ values need to be determined for the Mo isotopes.

The present IBA-2 calculations were initiated to see whether or not the ground-state two-neutron transfer strengths observed for the Mo nuclei can be reproduced. No attempt was made to fine tune the parameters, especially since it was recently shown in a Pt(*t,p*) study²⁹ that ground-state two-neutron transfer strengths are relatively insensitive to parameters of the IBA or other models. A question to be resolved, however, was what number of proton bosons, N_π , characterize the Mo isotopes. N_π is usually taken as the number of pairs of valence protons, so for Mo N_π would equal 4, representing eight protons from $Z = 50$. However, $Z = 40$ is a reasonably good proton subshell closure, so we have also done calculations for Mo with $N_\pi = 1$. Our parameter choices are summarized in Fig. 11.

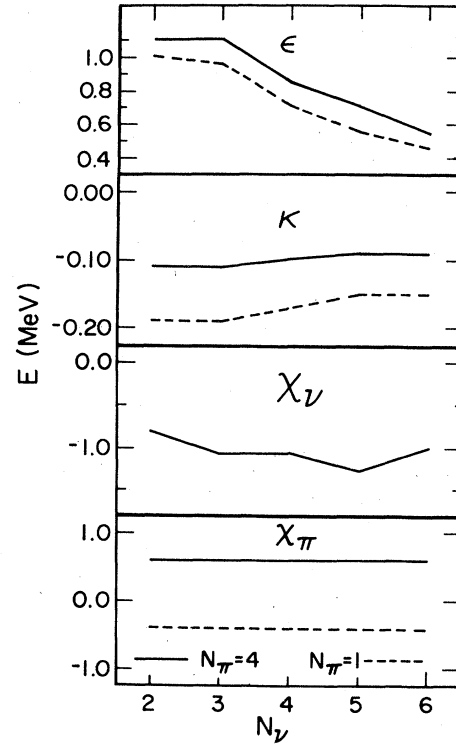


FIG. 11. Parameters used in the present IBA-2 calculations, plotted as a function of neutron boson number N_ν . The solid lines are values used in the $N_\pi = 4$ calculations; the dashed lines for $N_\pi = 1$. Values for χ_ν were taken from Ref. 27. The χ_π value for the $N_\pi = 4$ calculations is a natural extrapolation of values used for Ru and Pd calculations in Ref. 27; the $N_\pi = 1$ χ_π value is of opposite sign, as expected from Ref. 28.

As seen in Fig. 12, the present IBA-2 calculations are in reasonable agreement with the known systematics of the lowest 2^+ and 4^+ states for both the $N_\pi = 4$ and $N_\pi = 1$ calculations. Clearly, the strong trend of the falling 2_1^+ state is reproduced. The main problem in the energy predictions in the present calculations is that we cannot reproduce the location of the lowest excited 0_2^+ state.

The comparison between IBA predicted and empirical ground-state ϵ values is shown in Fig. 13, and no agreement is seen. The predictions were normalized to the $^{96}\text{Mo}(t,p)^{98}\text{Mo}$ ground-state value, but any other normalization would still not reproduce the data, which are clearly down sloping, while the calculations are clearly up sloping.

The key to understanding the reasonable fit to the energy spectra, while no agreement is found for two-neutron transfer strengths, may be in the 0_2^+ state. This state may be an intruder configuration,³⁰ a state from outside the IBA framework,

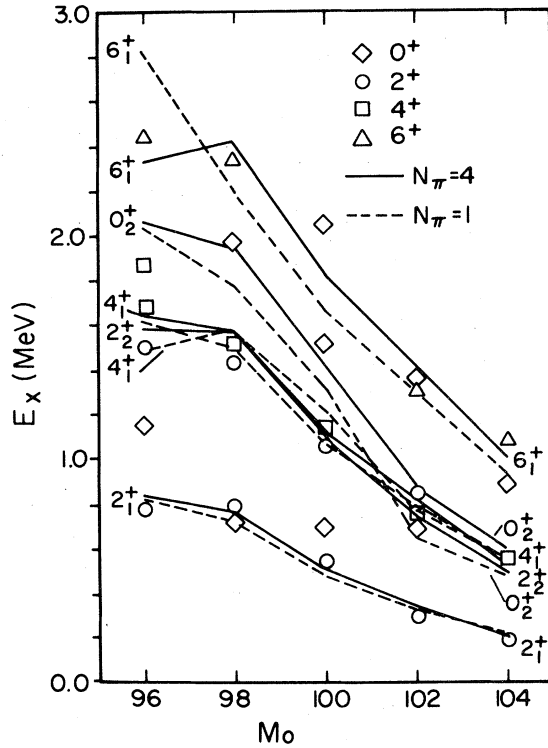


FIG. 12. Comparison of empirical energy systematics for 2_1^+ , 2_2^+ , 4_1^+ , 6_1^+ , and 0_2^+ states in $^{96-104}\text{Mo}$ and IBA-2 calculations for $N_\pi=4$ (solid) and $N_\pi=1$ (dashed). The calculations are discussed in the text and Fig. 11. The data are taken from Ref. 8 and the present work.

such as a particle-hole excitation across the $Z=40$ proton subshell closure. In IBA language, this would mean that the boson number N_π would not uniquely characterize the level spectra, but rather states with different numbers of bosons would coexist in the same nucleus, and mixing between the configurations would result. Recently, this approach was used in a study of $^{184-188}\text{Hg}$ and the coexistence of vibrational states and rotational bands in these nuclei was reproduced.³¹

Concurrent with the present study, calculations of the Mo isotopes have been performed³⁰ using the method of Ref. 31. The ground-state regions of the lighter Mo isotopes, such as for ^{96}Mo , are predominantly due to $N_\pi=1$ configurations and, hence, are fairly spherical in structure. For the heavier Mo isotopes, such as ^{104}Mo , the ground-state regions are predominantly $N_\pi=3$. [$N_\pi=3$ from the particle boson above $Z=40$ plus two bosons from

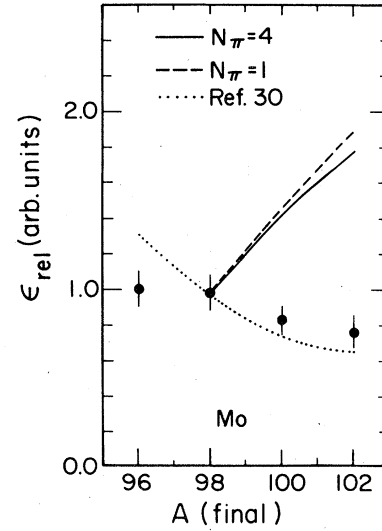


FIG. 13. Comparison between empirical and IBA calculated ground-state relative ϵ values in $\text{Mo}(t,p)$. The ϵ values are plotted versus the mass of the final nucleus. The empirical ϵ values were taken from Table XI with a 10% relative error; the calculations were arbitrarily normalized to the $^{96}\text{Mo}(t,p)^{98}\text{Mo}$ g.s. value. The solid and dashed curves are our IBA-2 calculations with $N_\pi=4$ and $N_\pi=1$, respectively. The dotted curve is the extended IBA calculation from Ref. 30.

the particle-hole (boson) excitation across the subshell closure.] The intruder state in the lighter Mo isotopes would be a predominantly $N_\pi=3$ excitation, and in the heavier isotopes the intruder would be $N_\pi=1$. The transition between $N_\pi=1$ and $N_\pi=3$ ground-state configurations then occurs around $A=100$. Since mixing is included in these calculations, an $N_\pi=3$ component would also occur in the ^{96}Mo ground state and an $N_\pi=1$ component in the ^{104}Mo ground state. These calculations³⁰ were able to reproduce the trends in the low-lying excitations and, in particular, reproduced the energy systematics of the 0_2^+ states.

Obtaining two-neutron transfer strengths in the extended IBA-2 calculations is not as straightforward as calculating energy values and γ -ray transition probabilities. As noted in earlier studies of two-neutron transfer in the IBA framework,^{32,33} different limiting symmetries have different analytical expressions for the transfer strengths. An initial attempt to study the two-neutron transfer strengths in $\text{Mo}(t,p)$ used the following relation³⁰

$$I(N_\nu \rightarrow N_\nu + 1) \cong \alpha_\nu^2 (N_\nu + 1)(\Omega_\nu - N_\nu) \left\{ [c_1(N_\nu) c_1(N_\nu + 1)]^2 + \frac{2N + 3}{3(2N + 1)} [c_3(N_\nu) c_3(N_\nu + 1)]^2 \right\}, \quad (8)$$

where Ω_ν is the degeneracy of the neutron shell, $c_1(N_\nu)$ is the amplitude of the $N_\pi=1$ component in the ground state of the nucleus with N_ν , and $c_3(N_\nu)$ is the amplitude of the $N_\pi=3$ component. A comparison between the relative intensities predicted by Eq. (8) and our Mo(*t,p*) ϵ values is shown in Fig. 13. The agreement is quite good between these extended IBA-2 predictions and our empirical values, indicating that these extended calculations are able to reproduce the change in the ground-state configurations in the Mo isotopes.

VI. CONCLUSIONS

This systematic study of the Mo isotopes by the (*t,p*) reaction has clearly shown the effect of the onset of a phase transition which occurs near $A=100$. The lighter Mo isotopes compare favorably with the Zr isotopes and a shell-model description. As more neutrons are added there is a distinctive change between the two elements, and the strong $d_{5/2}$ subshell closure at $N=56$ seen in Zr is completely washed out in the Mo isotopes by the onset of the transition. Finally, in the heavier Mo isotopes there is increasing $L=0$ strength to excited states, which is a characteristic sign of a nuclear phase transition.

Federman and Pittel have suggested⁹ that the onset of deformation in the heavier Zr and Mo nuclei may be due to the increasing interaction between the $g_{9/2}$ proton and $g_{7/2}$ neutrons. Certainly the $g_{7/2}$ neutron strength is occurring lower in excitation energy and becoming a dominant part of the low-lying spectra of the odd nuclei. This may indeed explain the difference between Zr and Mo, where the latter has two more protons to interact. It would be extremely useful to have a more quan-

titative measure of the importance of this degree of freedom in understanding the properties of these nuclei.

Until recently the interacting boson approximation model has not been applied in nuclei only one proton pair removed from closed shells. Our present calculations within the standard IBA-2 framework indicate the limits to which this model can be applied in the molybdenums, which are close to a proton subshell closure. Concurrent to the present study, however, considerable work has gone into understanding intruder configurations^{30,31} in the IBA framework, and these extended IBA calculations have been successful in explaining the structure of Mo and Hg isotopes. It would be interesting to see if similar techniques can be successfully applied to other nuclei in the Zr-Mo region.

ACKNOWLEDGMENTS

We are very grateful to S. Orbesen who assisted us in the experiment, to Judith Gursky who prepared some of the targets, and to Dr. J. Wilhelmy who lent us the remainder. The work of the Van de Graaff staff under trying circumstances is deeply appreciated. One of us (F.A.S.) would like to express her deep appreciation to her colleagues at Los Alamos for their hospitality. We would like to thank Prof. F. Iachello for discussing recent developments in the IBA model and M. Cunningham for assisting in our calculations. We are also grateful to Dr. M. Sambataro and Dr. G. Molnar for providing results on their extended IBA calculations prior to publication. This work was done under the auspices of the U. S. Department of Energy.

*Physics Department, University of Pennsylvania, Philadelphia, Pennsylvania 19104.

†Present address: Wright Nuclear Structure Laboratory, Yale University, New Haven, Connecticut 06511.

¹E. R. Flynn, R. E. Brown, J. A. Cizewski, J. W. Sunier, W. P. Alford, E. Sugarbaker, and D. Ardouin, *Phys. Rev. C* **22**, 43 (1980).

²R. F. Casten, E. R. Flynn, O. Hansen, and T. J. Mulligan, *Nucl. Phys.* **A184**, 357 (1972).

³S. Takeda, S. Yamaji, K. Matsuda, I. Kohno, N. Nakanishi, Y. Awaya, and S. Kusuno, *J. Phys. Soc. Jpn.* **34**, 1115 (1973).

⁴H. L. Sharma, R. Seltz, and N. M. Hintz, *Phys. Rev.*

C **7**, 2567 (1973).

⁵H. Taketani, M. Adachi, M. Ogawa, K. Ashibe, and T. Hattori, *Phys. Lett.* **27**, 520 (1971).

⁶J. B. Ball, R. L. Auble, J. Rapaport, and C. B. Fulmer, *Phys. Lett.* **30B**, 533 (1969).

⁷E. Cheifetz, R. C. Jared, S. G. Thompson, and J. B. Wilhelmy, *Phys. Rev. Lett.* **25**, 38 (1970).

⁸K. Sistemich, W. D. Lauppe, H. Lawin, H. Seyforth, and B. D. Kern, *Z. Phys. A* **289**, 225 (1979).

⁹P. Federman and S. Pittel, *Phys. Rev. C* **20**, 820 (1979).

¹⁰A. Arima and F. Iachello, *Phys. Rev. Lett.* **35**, 1069 (1975).

¹¹E. R. Flynn, D. D. Armstrong, J. G. Beery, and A. G.

- Blair, Phys. Rev. 182, 1113 (1969).
- ¹²S. D. Orbesen, J. D. Sherman, and E. R. Flynn, Los Alamos Scientific Laboratory Report LA-6271-MS, 1976.
- ¹³E. R. Flynn, S. D. Orbesen, J. D. Sherman, J. W. Sunier, and R. W. Woods, Nucl. Instrum. Methods 128, 35 (1975).
- ¹⁴P. D. Kunz (unpublished).
- ¹⁵F. G. Perey, Phys. Rev. 131, 745 (1963).
- ¹⁶E. R. Flynn and O. Hansen, Phys. Lett. 31B, 135 (1970).
- ¹⁷S. Yoshida, Nucl. Phys. 33, 685 (1962).
- ¹⁸R. C. Diehl, B. L. Cohen, R. A. Moyer, and L. H. Goldman, Phys. Rev. C 1, 2132 (1970).
- ¹⁹P. K. Bindal, D. H. Youngblood, R. L. Kozub, and P. H. Hoffmann-Pinther, Phys. Rev. C 12, 1826 (1975).
- ²⁰E. R. Flynn, J. G. Beery, and A. G. Blair, Nucl. Phys. A218, 285 (1974).
- ²¹J. B. Ball and K. H. Bhatt, quoted in Ref. 20.
- ²²S. S. Ipson, K. C. McLean, W. Booth, J. G. B. Haigh, and R. N. Glover, Nucl. Phys. A253, 189 (1975).
- ²³E. R. Flynn, G. Igo, P. D. Barnes, D. Kovar, D. Bes, and R. A. Broglia, Phys. Rev. C 3, 2371 (1971).
- ²⁴R. E. Anderson, J. J. Kraushaar, I. C. Oelrich, R. M. DelVecchio, R. A. Naumann, E. R. Flynn, and C. E. Moss, Phys. Rev. C 15, 123 (1977).
- ²⁵H. Nann, E. R. Flynn, D. L. Hanson, and S. Raman, Phys. Rev. C 18, 2511 (1978).
- ²⁶*Table of Isotopes*, 7th ed., edited by C. M. Lederer and V. S. Shirley (Wiley, New York, 1978).
- ²⁷P. van Isacker and G. Puddu, Nucl. Phys. A348, 125 (1980).
- ²⁸A. Arima, T. Otsuka, F. Iachello, and I. Talmi, Phys. Lett. 66B, 205 (1977); T. Otsuka, A. Arima, F. Iachello, and I. Talmi, Phys. Lett. 76B, 139 (1978).
- ²⁹J. A. Cizewski, E. R. Flynn, R. E. Brown, D. L. Hanson, S. D. Orbesen, and J. W. Sunier, Phys. Rev. C 23, 1453 (1981).
- ³⁰M. Sambataro and G. Molnar (unpublished).
- ³¹P. D. Duval and B. R. Barrett, Phys. Lett. 100B, 223 (1981).
- ³²A. Arima and F. Iachello, Phys. Rev. C 16, 2085 (1977).
- ³³J. A. Cizewski, E. R. Flynn, R. E. Brown, and J. W. Sunier, Phys. Lett. 88B, 207 (1979).